

Examining the Impact of Blur on Recognition by Convolutional Networks

Igor Vasiljevic
University of Chicago
ivasiljevic@uchicago.edu

Ayan Chakrabarti
TTI-Chicago
ayan@ttic.edu

Gregory Shakhnarovich
TTI-Chicago
greg@ttic.edu

Abstract

State-of-the-art algorithms for semantic visual tasks—such as image classification and semantic segmentation—are based on the use of convolutional neural networks. These networks are commonly trained, and evaluated, on large annotated datasets of high-quality images that are free of artifacts. In this paper, we investigate the effect of one such artifact that is quite common in natural capture settings—blur. We show that standard pre-trained network models suffer a significant degradation in performance when applied to blurred images. We investigate the extent to which this degradation is due to the mismatch between training and input image statistics. Specifically, we find that fine-tuning a pre-trained model with blurred images added to the training set allows it to regain much of the lost accuracy. By considering different combinations of sharp and blurred images in the training set, we characterize how much degradation is caused by loss of information, and how much by the uncertainty of not knowing the nature and magnitude of blur. We find that by fine-tuning on a diverse mix of blurred images, convolutional neural networks can in fact learn to generate a blur invariant representation in their hidden layers. Broadly, our results provide practitioners with useful insights for developing vision systems that perform reliably on real world images affected by blur.

1. Introduction

Recent years have seen tremendous progress in the development of computer vision algorithms for semantic tasks such as image classification [8, 11, 20], object detection [7, 17], and semantic segmentation [2, 15], with most modern state-of-the-art methods based on convolutional neural networks. These methods owe much of their success to the availability of large image datasets [3, 5] with ground truth data collected through human annotation. To build datasets at such scales, researchers have had to rely on images freely shared by regular users. But the statistics of photographs people upload to a photo-sharing website

could be different from those a vision system encounters while operating. This is a concern since modern methods are not only trained, *but also evaluated*, on these datasets.

In particular, there is significant potential for a disparity between the low-level statistics of images a vision algorithm receives as training input, and publicly shared photographs. This is because users tend to upload photographs, often selected from among multiple trials of capturing the same object, that are high-quality and free of artifacts—*e.g.* saturation, distortions, and motion and defocus blur. In this paper, we concentrate on blur, since it is quite easy to end up with a blurred image even with a high-quality camera, especially in a setting where the user is not concerned about image quality (*e.g.*, when the image is being taken for a vision application, rather than for photography), or when the image is being captured automatically by a device or robot. We are also motivated by the recent findings of Dodge and Karam [4], who show that existing image classification networks exhibit significant lower accuracies when evaluated on images with Gaussian blur.

We conduct a systematic survey of the effect of blur on the performance of convolutional neural networks for image recognition. We begin by evaluating pre-trained network models on images degraded with a range of different blurs, and reach a similar conclusion as [4]: state-of-the-art networks trained on sharp image datasets make unreliable predictions when evaluated on blurry images. Moreover, we find that these unreliable predictions are accompanied by underlying high-entropy class distributions (*e.g.*, see Fig. 1). This is encouraging since it can allow vision systems using these networks to account for the low-confidence of their predictions (and, say, ask the user to take another image).

We also examine the interaction between blur and multi-scale processing: applying the trained network at multiple resized versions of the input image is commonly used as a way to build robustness to variations to the relative scale of objects in the image. However, we find that the inclusion of larger sized versions is detrimental when blur may be present, since it exaggerates the effect of such blur.

Next, we demonstrate that much of this performance degradation is an artifact of these models being trained only

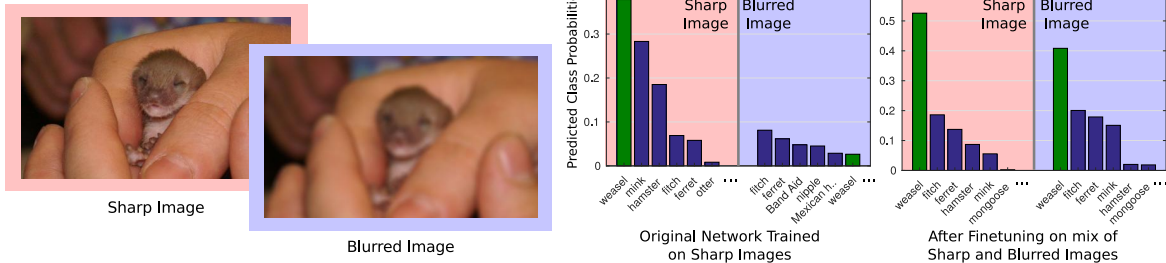


Figure 1. State-of-the-art image classification networks like VGG-16 [20] perform poorly on blurred input (left), when using model weights trained on high-quality sharp image datasets (center). However, while they often make erroneous predictions in terms of the most likely classes for a blurred image, they do so with lower confidence—producing distributions that are higher-entropy than those for sharp images. However, this drop in performance is largely an artifact of being trained without any blurred examples. We find that by fine-tuning the model on a mix of blurred and sharp images for just a few epochs, allows it to perform well on both sharp and blurred inputs (right).

on sharp images, rather than due to an intrinsic absence of information in blurry images, or a deficiency in the networks’ architectures. By fine-tuning with a mix of blurry and sharp images for only three epochs, we find that a network trained only on sharp images is able to recover most of its lost accuracy on blurry images. In these experiments, we also investigate the role of uncertainty about the nature of blur in the input, by fine-tuning over different distributions of blur. We find that a model fine-tuned with a fairly diverse range of blurs performs reasonably well, and is only slightly less accurate than a network that is trained and evaluated on a single blur level (which in-turn performs worse on other blur levels). This demonstrates the ability of the network to learn a level of blur *invariance*, which we further examine by comparing the activations for a sharp and blurred image pair, at different layers in the network. Finally, in addition to image classification, we find that these observations also largely carry over to the task of semantic segmentation, where fine-tuning with blurry images is able to improve accuracy in both identifying and localizing objects in blurred images.

Broadly, our findings reinforce the fact that convolutional neural networks are resilient—when presented with an out-of-distribution input, they are able to signal a low-confidence in their predictions, and are quickly able to adapt when provided with additional training data, without any modification in architecture. Moreover, our experiments provide useful insight for designing vision systems that need to reason with potentially blurred images in a practical, non-idealized, setting.

2. Background & Related Work

Blur is a degradation in image quality caused by camera sensor pixels averaging light from overlapping regions in the scene, typically due to defocus or motion in the capture interval. Often, an observed blurry image can be well-modeled as a convolution of a *latent* sharp image (*i.e.*, the image that would have been captured in the absence of blur),

and a blur kernel or point-spread-function. In the case of defocus blur, this kernel is an image of the lens aperture (typically a disk) scaled by a factor proportional to the distance of the imaged object from the focal plane. For motion blur, it is the projection of the moving object or camera’s trajectory during the exposure interval. Both kinds of blur kernels are “low-pass” filters, *i.e.*, they lead to a loss or attenuation of high-frequency image detail.

Reversing the effect of blur to obtain a sharp image from a blurred observation is an ill-posed inverse problem, especially when the blur is unknown. Graphics and vision researchers have made significant progress on this problem across the last decade [6, 12, 14, 24]—including with recent neural network-based methods [1, 18, 19, 23]. Nevertheless, image deblurring remains a challenging and computationally expensive task. However, our goal in this paper is different. Instead of processing blurred images to recover sharp photographs for human consumption, we seek to understand, and ameliorate, the effect of using these images as input to algorithms for recognition.

Nearly all state-of-the-art computer vision algorithms for semantic visual tasks rely on the use of convolutional neural networks [2, 7, 8, 11, 15, 17, 20]. Critical to their success is the ability to train on large annotated datasets, like Imagenet [3] and Pascal VOC [5]—both of which contain photographs downloaded from the photo sharing website [flickr.com](http://www.flickr.com). Therefore, these datasets contain images that users—amateurs and professional photographers alike—have *chosen* to upload, and are consequently of high-quality with few artifacts.

Since standard recognition benchmarks perform their evaluation on held-out portions of the same dataset, the reported performance of state-of-the-art algorithms can at best be interpreted to accurately characterize their expected accuracy on similar high-quality image data. To address this, Dodge and Karam [4] recently carried out an evaluation of standard neural network-based methods for image classification on images degraded by Gaussian blur, and reported a

significant drop in classification accuracy. Karahan *et al.* [9] perform a similar evaluation for face-recognition, while Ullman *et al.* [22] contrasted the drop in the accuracy of computational recognition to that of humans.

We too study the classification accuracy of pre-trained networks on blurry images—for a larger family of realistic blur kernels—and find a similar drop in performance. However, we find that while networks trained on sharp images make erroneous predictions on blurred input, they do so with low-confidence. Moreover, we show that this drop is mainly caused by the high-quality bias in the images used for training these networks, and that performance on blurred images can be significantly improved with adding such images to the training set—without requiring a change in their architecture. We also examine the ability of the networks to learn to perform consistently across a diversity of possible blurs, and find that these networks are able to do so by learning feature representations that are invariant to blur. Finally, we investigate the impact of blur on a different task—semantic segmentation. We find that blur affects the ability of pre-trained networks to both identify and localize objects, but that like for classification, this ability can be recovered to a considerable extent by training with blurred images.

Therefore, we find that convolutional neural networks can succeed despite degradations in image quality from blur. This is consistent with such networks having been used quite successfully for the classification of very low-quality images, albeit on smaller benchmarks—*e.g.*, CIFAR-100 [10] that contains extremely low-resolution images of size 32×32 . In this context, recently Peng *et al.* [16] explored the potential of jointly training with high-resolution images to boost performance on low-resolution inputs. Our work also demonstrates the success of neural networks in the face of lower image quality, with joint training with images of varying quality, to deal with degradation due to optical blur for large-scale visual recognition.

Finally, it is worth noting here the work of Szegedy *et al.* [21], who found that specific small-magnitude perturbations could cause network models to produce erroneous estimates. However, these perturbations were not random, and determined through an optimization process. In contrast, our focus is on errors due to a naturally prevalent form of image degradation—blur.

3. Imagenet Classification on Blurred Images using Pre-trained Network Models

We begin by evaluating the performance of state-of-the-art convolutional neural network models—VGG-16 [20] and ResNet [8]—on blurred versions of the Imagenet [3] standard 2012 validation set. These models were trained on the Imagenet training set that comprised of largely sharp, high-quality images. We generate the blurred versions of the validation set by convolving the original sharp images

Scale	128	256	256+512	512
Sharp	76.07%	90.88%	92.17%	90.76%
Defocus r=2 (D2)	74.83%	88.06%	89.00%	85.43%
Defocus r=4 (D4)	68.48%	81.48%	80.93%	66.86%
Defocus r=6 (D6)	61.03%	72.69%	67.86%	40.64%
Defocus r=8 (D8)	53.34%	60.97%	51.40%	22.52%
Horiz. length=4	75.37%	89.11%	90.04%	86.59%
Horiz. length=8	70.73%	83.32%	82.77%	71.50%
Vert. length=4	75.57%	88.79%	89.84%	86.19%
Vert. length=8	70.75%	82.51%	81.86%	69.20%
Gaussian $\sigma = 4$	56.34%	62.38%	49.80%	19.76%
Gaussian $\sigma = 8$	30.15%	17.39%	11.37%	3.41%

Table 1. Top-5 Accuracy on sharp and blurred versions of Imagenet Val images, using the original VGG-16 network that was trained on sharp images. We report performance for applying the network at different scales, where the input images were resized to make their smaller side fit the indicated scale value.

with a range of different blur kernels.

Note that both [8] and [20] resize their input to one or more pre-determined scales (to match their smaller side to the scale value), and then compute class probability distributions by feeding this resized image to their network model. However, images in the Imagenet dataset are of various sizes. Therefore, rather than blur the original images directly, we first resize the image to a fixed scale (384 in our experiments) and then convolve the result with the blur kernel. This ensures that the effective blur for a chosen kernel is consistent across images, irrespective of their original size. We then quantize the blurred intensities to form 8-bit images, which are then further rescaled and fed into the classification networks.

We begin by reporting the performance VGG-16 network [20] for a diverse set of blur kernels in Table 1. We consider disk kernels of different radii r (that have a constant value within their radius, and zero outside) to simulate defocus blur, and with horizontal and vertical box kernels of single pixel width and different lengths that correspond to motion blur (for uniform linear motion). Like [4], we also report results on blurring with Gaussian kernels of different standard deviations σ . All kernels are normalized to be unit sum, *i.e.*, they have a “DC value” of one.

We use the original network model provided by the authors of [20], who reported best performance by applying the network at two scales—256 and 512—where at each scale, the network (which has a receptive field of 224×224) was applied in a fully-convolutional way on all crops (with the network’s natural stride of 32). The log-probabilities from all crops from all scales were then averaged. We adopt a similar methodology, but also apply the network at different individual scales—128, 256, and 512—as well as the

suggested combination of 256 and 512. To apply the network at the scale of 128, which is smaller than the network’s receptive field, we zero-pad the *pool5* activations before passing them to the first fully connected layer.

Table 1 shows a clear drop in performance with increasing degrees of blur, for all types of blur kernels. Interestingly, this drop is steeper for bigger kernels in cases when the larger scale of 512 is included—by itself, or in combination with 256. Re-scaling to a larger size also increases the effective blur kernel size in the input to the network, and these results suggest that the benefits of robustness to object scale variation—the original motivation for multi-scale evaluation—are outweighed by the increasing effect of blur for larger kernels. In general, going to the lowest scale of 128 also hurts performance, likely because it causes a mismatch between object sizes seen during training (which was done with scales 256 and 512). The only exception are the results for Gaussian blur with $\sigma = 8$ —the largest kernel considered in our evaluation.

Figure 1 shows an example of the performance drop between sharp and blurred (with an $r = 8$ defocus kernel) versions of an image. We see that while the true class was correctly identified as most likely with high probability in the sharp image, it is relegated to sixth place in the blurred version. Note however that the class probabilities for even the most likely class are much lower, and the distribution is closer to uniform with high entropy. This phenomenon is not specific to this example—in Table 2, we report the average entropy (and cross-entropy) values of the predicted class distributions across the entire validation set, for sharp images, and two levels of defocus blur. Looking at the “Original” column of the table (which also includes results from fine-tuning the network discussed later in Sec. 4), we see that the drop in accuracy in Table. 1 is consistently accompanied by a significant increase in entropy. Therefore, while the model makes inaccurate predictions when used on unexpectedly low-quality images (compared to its training set), it does so with low-confidence.

We also report classification results on blurred images with the more recent ResNet [8] architecture in Table 3, considering various levels of defocus blur. We use the pre-trained model weights provided by the authors, and apply the network on five crops with two different scale settings: 256, and a combination of 256 and 512. We find that while the absolute accuracies of the ResNet model are slightly higher—for both sharp and blurred images—than for VGG-16, there is a similar drop in accuracy with increasing blur. This confirms that the drop in accuracy due to blur is not peculiar to the VGG-16 architecture.

4. Improving Performance with Fine-tuning

Next, we investigate how much of the performance degradation seen in the previous section is simply due

	Entropy		Cross-Entropy	
	Original	Fine-tuned	Original	Fine-tuned
Sharp	1.1837	1.1215	1.2060	1.1449
Blur D4	2.6131	1.3629	2.6513	1.3882
Blur D8	3.8021	1.6553	3.8654	1.6819

Table 2. Entropy and cross-entropy of predicted class-distributions on sharp Imagenet Val images and those blurred with defocus blur (of radius 4 and 8). Results are from applying (at scale 256) the original VGG-16 network, and the version fine-tuned with a mix of sharp and blurry (D2,4,6,8) images.

Scale	256	256 + 512
Sharp	92.89%	93.44%
Blur D2	90.40%	90.82%
Blur D4	85.20%	83.54%
Blur D6	77.07%	69.52%
Blur D8	66.14%	55.94%

Table 3. Top-5 Accuracies for the pre-trained **ResNet-51** model on sharp and blurred (with defocus blur of different radii) versions of Imagenet Val images. While the absolute accuracy values are a little higher than for VGG-16, we observe a similar drop in performance with increasing blur.

to a lack of blurred image samples in the training data. Other plausible explanations for this degradation include the possibility of a deficiency in the network architectures themselves (and not just their parameter values), or that blurred images simply lack the required semantically discriminative information needed to make accurate predictions. We largely rule out these possibilities by showing that fine-tuning the original VGG-16 for a small number of epochs on different combinations of sharp and blurred images nearly closes the performance gap caused by blur.

We begin with the weights in the pre-trained model, and then fine-tune with two epochs at a learning rate of 10^{-3} followed by one epoch at 10^{-4} , with a momentum value of 0.9 and a batch-size of 128. We construct our training batches from the official Imagenet-2012 training set, shuffling the set at the beginning of each epoch. We blur each image in the batch with a different selected kernel (or do not blur it at all) based on the chosen blur distribution. In different experiments, we resize the blurred image to either a fixed scale or a randomly selected scale, and then take a random 224×224 crop. We also randomly flip each image horizontally, and retain the dropout layers used for training the original model [20].

The original model was trained at multiple scales in order to build some degree of invariance to object scale [20]. However, as described in the previous section, image re-scaling interacts with blur. Therefore, most of our exper-

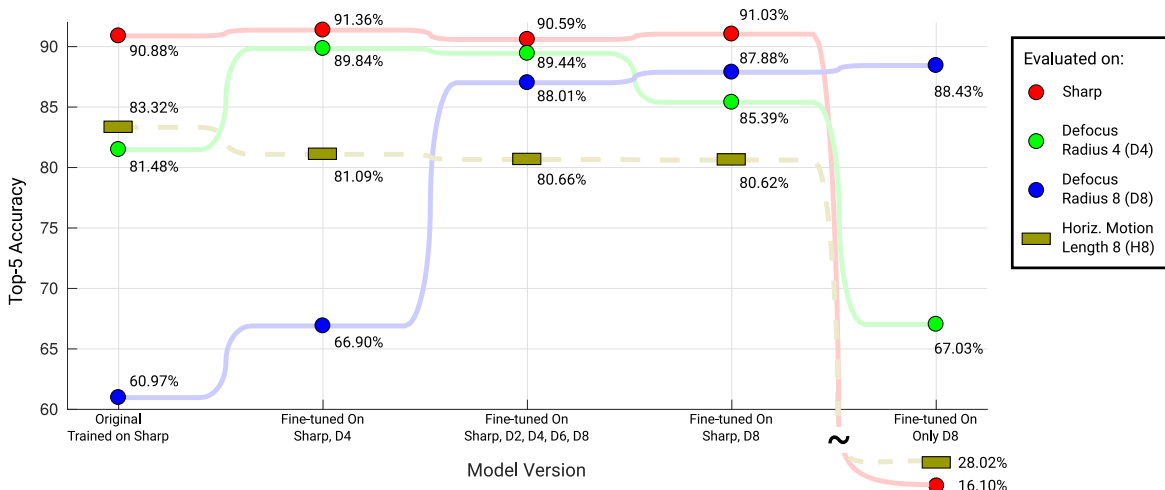


Figure 2. Classification performance on blurred images after fine-tuning VGG-16 with different combinations of blurred and sharp images. The different curves represent the Top-5 accuracy on different versions of the Imagenet validation set blurred with different kernels. The x-axis indexes different combinations of kernels used for fine-tuning, where the blur applied to each training image is uniformly sampled from the indicated set of blurs. Both training and evaluation are at scale 256. Fine-tuning with a uniform distribution across a wide range of blurs significantly improves performance of the network on blurred inputs, with negligible penalty on sharp images. There is also some generalization across blurs of the same type, where including either the D8 or D4 blur kernel in the fine-tuning set improves performance for the other, over the original model. However fine-tuning with defocus blurs degrades performance for motion-blurred images, suggesting no generalization across blur types. Moreover, it is possible to get minor benefits in performance for specific blurs by using a more restricted fine-tuning blur set. But in the case of training only with D8, this severely degrades accuracy for sharp and motion-blurred images.

iments involve re-scaling the blurred training images to a fixed scale, with only one setting involving multiple scales. We try to build object scale invariance, by considering different scales *prior* to the application of blur. Remember in our testing regime, a specific blur kernel is defined with respect to a fixed scale (of 384). So, we randomly re-scale training images to values around that scale (356, 384, and 410 in our experiments), and then apply blur. We then re-scale this blurred image to the target scale for the network by a factor equal to the ratio between the target training scale and the canonical blur scale (*i.e.*, 384). This achieves variation in object scale, while ensuring that in all training examples that were blurred with the same selected kernel and fed to the network at the same post-blur scale, the effective size of the blur kernel is consistent.

4.1. Fine-tuning with Different Blur Distributions

We begin by fixing the network scale at 256 (which yielded the best overall performance in Table 1), and run multiple fine-tuning experiments with different combinations of sharp and defocus blurred images. Figure 2 reports the performance of these different fine-tuned networks on different versions of the Imagenet validation set—including the original sharp images, and versions blurred by different defocus kernels. We also include results on versions blurred by one of the motion kernels, to examine the degree of generalization between different blur types.

We find that after fine-tuning with a diverse range of de-

focus blurs—specifically, a uniform mix of sharp images and those blurred with defocus blur of radii 2,4,6, and 8—the VGG-16 network begins to perform significantly better on blurred images, increasing Top-5 accuracy on the radius-8 defocus blurred images from 61% (for the original model) to 88%. Moreover, this comes at negligible cost to performance on sharp images, for which accuracy drops by less than a third of a percentage point. Indeed, fine-tuning with a mix of sharp images and only moderate (radius 4) defocus blur even leads to a slight improvement of half a percentage point in sharp image accuracy, suggesting that moderate blurring can act as a form of data augmentation.

We note that there is a certain amount of generalization among the different blur kernels. Including examples of radius-4 blur along with sharp images also improves performance on radius-8 blur, and vice-versa. However, this generalization does not appear to extend across blur types, and we see performance on motion-blurred images degrade over the original network with fine-tuning on all combinations of defocus blurs. We also see that if one has a-priori knowledge of the blur present in the input, there is some marginal improvement from using a network trained with a larger fraction of examples of that blur. However, the improvement is lower than the drop in performance for other blurs dropped from training. The most extreme example of this is when fine-tuning with all images blurred by the radius-8 defocus kernel, which severely degrades performance on sharp images. Indeed, this degradation is asymmetric—this

model’s accuracy on sharp images is lower than the original model’s accuracy on radius-8 defocus blur.

Therefore, training with a uniform distribution over possible blurs appears to be the right strategy (at least at our chosen scale and range of blurs), unless one has an accurate estimate of the blur affecting the input. Figure 1 includes the updated predicted class-distributions for our sharp and blurred example-pair from the model fine-tuned on the uniform blur set. We see the network now identifies the correct class in both the sharp and blurred version of the image, and indeed produces very similar class distributions for both. We also note that in addition to identifying the correct class in the blurred image, the network also makes this prediction with higher confidence. We report the average entropy of the class distributions from the fine-tuned model in Table 2, and find that fine-tuning not only improves the network’s accuracy on blurred images, but also systematically increases its confidence in these predictions.

4.2. Fine-tuning for Different Scales

Our decision to use a single scale of 256 to conduct the above fine-tuning experiments was based on the poorer performance of the original VGG-16 model at larger scales. However, a natural question is whether this trend continues to hold after fine-tuning. Therefore, we also finetune the model (beginning with the original weights) at a scale of 512, keeping the blur distribution fixed to the uniform setting (*i.e.*, with a mix of sharp images and blurred with kernels of radii 2-8). We then evaluate this model on the validation set, applying it at the 512 scale, and compare its performance to the 256-scale version in Table 4.

We find that while fine-tuning also significantly improves accuracy on blurred images at the 512 scale in comparison to the original model, these values are measurably lower than those of the model fine-tuned and applied at scale 256. Moreover, this improvement comes at a greater cost to performance on sharp images, with accuracy dropping by nearly three percentage points compared to the original model. Therefore, the relative advantage of using a lower scale persists even after fine-tuning.

Next, we consider the case of applying the network at both the 256 and 512 scales—this is the setting that achieves the highest accuracy on the sharp images with the original model. We test two versions of this approach. In the first, we fine-tune a single model on images randomly resized to one of these two scales (as was done for training the original model). As shown in Table 4, this model does better than the 512 scale model on both sharp blurred images, and slightly worse than the 256 scale model on blurred images.

In the second case, we apply separate networks at each scale for classification—using the models fine-tuned at only their respective scales. This approach finally catches up to the 256 scale fine-tuned model on blurred images, and ac-

Scale	Network	Sharp	D4	D8
256	Original	90.88%	81.48%	60.97%
	Fine-tuned	90.59%	89.44%	87.01%
512	Original	90.76%	66.86%	22.52%
	Fine-tuned	87.86%	85.99%	81.54%
256+512	Original	92.17%	80.93%	51.40%
	Fine-tuned (single network)	90.84%	89.17%	85.86%
	Fine-tuned (per-scale)	91.10%	89.80%	87.09%

Table 4. Top-5 Accuracies on sharp and blurry (defocus blur of radius 4 & 8) versions of Imagenet Val images, when applying the network at different scales. We show results from the original network, and versions that are fine-tuned (with mix of sharp and D2,4,6,8) at their respective scales. For the multi-scale 256+512 evaluation, we show results from a single network fine-tuned with both scales, and from applying a separate network at each scale.

tually outperforms it by half a percentage point on sharp images. This is likely because for sharp images, both scales participate in classification, while on blurred images, the 512-scale model outputs higher-entropy distributions causing the average to revert to the output of the 256-scale model. While the per-scale fine-tuning strategy does have slightly better overall performance (when considering both sharp and blurred images), this marginal improvement is unlikely to justify the additional memory requirement of storing two versions of the model for most applications.

4.3. Blur Invariance in Network Features

The fact that the fine-tuned model perform reliably on a wide range of blur sizes indicates that the network is able to learn to be invariant to blur. A natural question, then, is whether the network achieves this invariance early on, at the level of low-level image features in its initial layers, or at a more semantic level later in the network. We attempt to answer this question by looking at the similarity in activations of different layers of both the original and fine-tuned VGG models, when they are applied on the sharp and blurred versions of the same image.

Specifically, we consider the feature maps at the output of the five pooling layers in the VGG-16 network. We convert the feature vector at every location into a binary string representing whether the each feature channel had a positive or zero response. In Fig. 3, we visualize Hamming distances between corresponding binary strings produced from a sharp and blurred (by radius-8 defocus blur) versions of the same example image. We do this first at scale 256, for the original VGG-16 model, the model fine-tuned only on blurred images (defocus radius 8), and one on a mix of sharp and blurred (defocus radius 2-8) images. We find that

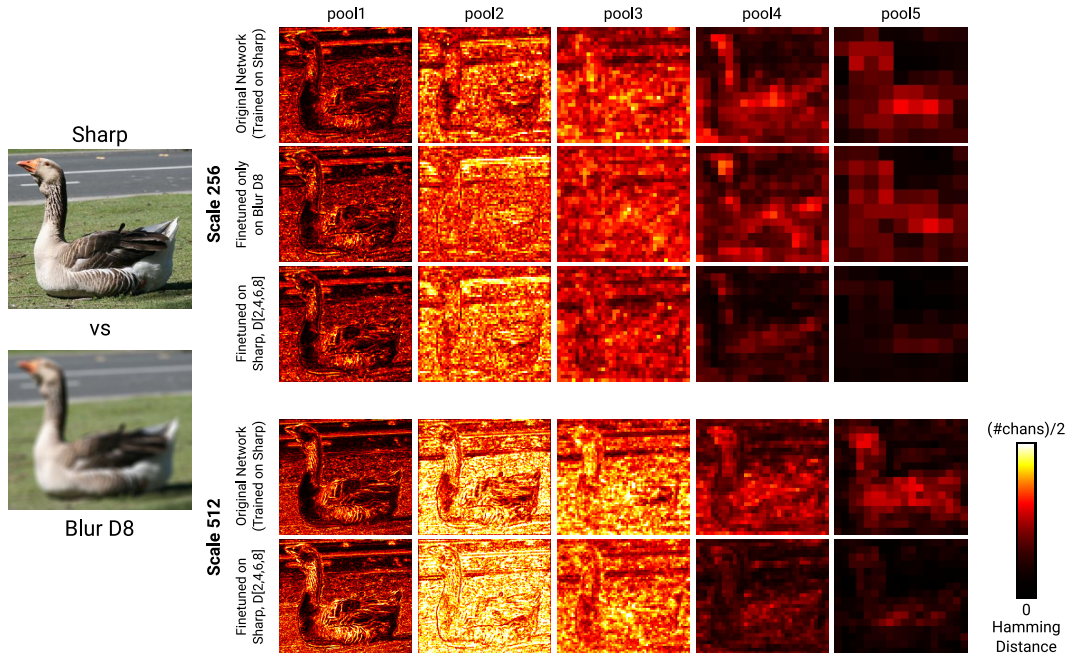


Figure 3. Disparity between corresponding layer activations on sharp and blurred versions of an example image, for different models at different scales. Each heat-map represents the Hamming distance between binarized feature vectors (representing whether each channel is positive or zero) at corresponding locations in the sharp and blurred inputs. We visualize these distance maps for the different pooling layers in the VGG-16 architecture, rescaling the maps for all layers to be the same size, and normalizing them by the number of feature channels. We see that the model fine-tuned (at scale 256) on a mix of sharp and blurred images produces feature activations at higher layers that are relatively invariant to the presence of blur in the input image. At scale 512, fine-tuning isn’t able to achieve a similar level of invariance—likely due to the larger effective blur size. This may partly explain the poorer performance at that scale in Table 4.

both the original model, and the one trained only on blurred images, yield different activations on the sharp and blurred inputs, at all layers. In contrast, the model fine-tuned on the mix of sharp and blurred images is able to achieve a reasonable amount of blur invariance, with low distances between sharp and blurred activations at the fifth (and to a lesser extent the fourth) pooling layer. Note that the disparity in activations in the initial layers of the network remains high. We believe that this may be because the initial layers have too small a view of the input to be able to reason about blur, or because blur invariance is easier to achieve at a higher semantic level than at the image feature level.

Figure 3 also compares the original and fine-tuned (with a uniform blur set) models at scale 512. Here we see that a fair amount of disparity persists at the final pooling layer even after fine-tuning, and is consistent the 512 scale model’s poorer performance in Table 4. Since the effective blur kernel size is twice as large at scale 512 than scale 256, this disparity may well be due to input view size at even the last pooling layer’s being insufficient in this case.

5. Semantic Segmentation on Blurred Images

In this section, we examine whether our observations from the previous sections on image classification carry

over to a different semantic visual task—semantic segmentation. The effect of blur for this task is especially interesting, since low-level image detail, which is attenuated by blurring, plays a larger role—in addition to recognizing the identity of an object, a successful segmentation algorithm must also be able to localize it precisely at the pixel level.

We perform our experiments using the *Zoomout* method of Mostajabi *et al.* [15] on the VOC2012 benchmark [5]. This method uses a VGG-16 model pre-trained on Imagenet, and learns a per-pixel classifier for object class on top of a feature-vector constructed from activations from multiple layers. This classifier is trained in conjunction with fine-tuning of the VGG-16 layers. We begin by evaluating the effect of blur on model weights made available by the authors, that was trained on (largely sharp) images in the VOC training set and from the COCO segmentation database [13]. We only consider different degrees of defocus blurs in this case, and use a similar methodology as before for generating blurred versions of the VOC2012 validation images, *i.e.*, after resizing to a fixed scale of 384. However, since [15] uses anisotropic scaling to create the input (distorting the aspect-ratio) to its network, we perform scaling by matching the geometric mean, instead of the minimum, of width and height to 384.

Table 5 reports values of the standard mean Intersection-

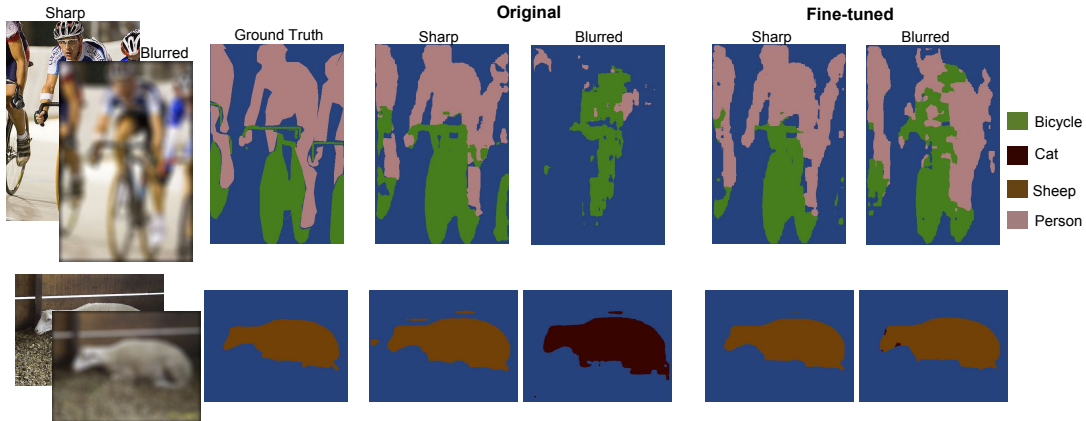


Figure 4. Semantic segmentation results on sharp and blurred images using the Zoomout [15] network. We show results from the original model trained on sharp images, and one fine-tuned on a mix of sharp and blurred examples. Blur causes both errors in localization (top-row) and class identification (bottom-row) in the original model, but these errors are considerably reduced by fine-tuning.

over-Union (mIOU) metric on sharp and blurred versions of the VOC validation set. In order to separately evaluate the degradation in boundary localization, we also report a version of this metric computed only at locations within a four pixel distance of class boundaries. Like for classification, we note that the pre-trained model suffers significant degradation in the presence of blur. However, this degradation appears to affect both general accuracy and localization. We see examples of this in Fig. 4 where in one instance, the model is able to identify object classes correctly in the blurred image, but performs a poorer segmentation between the classes and the background than in the sharp version. In the other example, the network produces a fairly high-quality segmentation of the foreground from the blurred image, but mis-identifies its class.

Next, we evaluate the effect of fine-tuning the model with a mix of sharp and blurred images. We fine-tune only on the VOC training set, for six epochs at a learning rate of 10^{-4} , and two at a rate of 10^{-5} . The performance of this fine-tuned model is also reported in Table. 5. Like for image classification, we find that performance on blurred images improves with fine-tuning. Moreover, this improvement is seen in both general accuracy, as well as in regions close to boundaries. In the first example in Fig. 4, we see that the fine-tuned network improves its ability to localize class boundaries on the blurred input, and is able to switch to the correct class label in the second input.

However, in contrast to classification, we find that the gap between sharp and blurred image performance remains larger after fine-tuning, and the improvements at a greater cost to sharp image performance. We believe this is due to the fact that this task is fundamentally more affected by blur. It requires identifying and separating objects, and the smearing of intensities across object boundaries due to blur makes this separation harder.

	Original		Fine-tuned	
	All	Boundaries	All	Boundaries
Sharp	70.0%	55.5%	68.2%	54.2%
Blur D2	63.8%	47.0%	64.8%	50.2%
Blur D4	50.0%	33.5%	58.7%	44.2%
Blur D6	35.2%	21.8%	51.3%	37.3%
Blur D8	23.1%	13.2%	43.0%	30.5%

Table 5. mIOU accuracy on sharp and blurred versions of the VOC val images, using the Zoomout network with original and fine-tuned weights. In addition to average accuracy over all pixels, we also separately calculate mIOU over pixels that within a four pixel neighborhood of class boundaries.

6. Conclusion

State-of-the-art network models trained on high-quality image datasets make unreliable, albeit low-confidence, predictions when they encounter blur in their inputs. In this work, we found that much of this unreliability is due to an inability to generalize from their sharp training sets, and that fine-tuning these models for a relatively small number of epochs with blurred training examples significantly improves their performance on blurry inputs. Moreover, we showed that standard architectures are able to deal with a diverse range of blurs, by learning to produce internal representations that are invariant to blur.

Our analysis provides insights for building and deploying vision systems in real-world settings where blur may be present. More broadly, we expect our findings to be relevant for other forms of imaging non-idealities beyond blur. In future work, we plan to explore un-supervised ways of achieving robustness to image artifacts—*e.g.*, when we have access to examples of distorted natural images, but not to a precise model for the distortion.

References

- [1] A. Chakrabarti. A neural approach to blind motion deblurring. In *Proc. ECCV*, 2016. 2
- [2] L.-C. Chen, G. Papandreou, I. Kokkinos, K. Murphy, and A. L. Yuille. Deeplab: Semantic image segmentation with deep convolutional nets, atrous convolution, and fully connected CRFs. In *Proc. CVPR*, 2016. 1, 2
- [3] J. Deng, W. Dong, R. Socher, L.-J. Li, K. Li, and L. Fei-Fei. ImageNet: A Large-Scale Hierarchical Image Database. In *Proc. CVPR*, 2009. 1, 2, 3
- [4] S. Dodge and L. Karam. Understanding how image quality affects deep neural networks. In *Proc. International Conference on Quality of Multimedia Experience*, 2016. 1, 2, 3
- [5] M. Everingham, L. V. Gool, C. K. I. Williams, J. Winn, and A. Zisserman. The PASCAL Visual Object Classes (VOC) Challenge. *IJCV*, 2010. 1, 2, 7
- [6] R. Fergus, B. Singh, A. Hertzmann, S. T. Roweis, and W. T. Freeman. Removing camera shake from a single photograph. *SIGGRAPH*, 2006. 2
- [7] R. Girshick, J. Donahue, T. Darrell, and J. Malik. Rich feature hierarchies for accurate object detection and semantic segmentation. In *Proc. CVPR*, 2014. 1, 2
- [8] K. He, X. Zhang, S. Ren, and J. Sun. Deep residual learning for image recognition. In *Proc. CVPR*, 2016. 1, 2, 3, 4
- [9] S. Karahan, M. K. Yildirim, K. Kirtac, F. S. Rende, G. Butun, and H. K. Ekenel. How image degradations affect deep CNN-based face recognition? *arXiv:1608.05246*, 2016. 3
- [10] A. Krizhevsky and G. Hinton. Learning multiple layers of features from tiny images. 2009. 3
- [11] A. Krizhevsky, I. Sutskever, and G. E. Hinton. Imagenet classification with deep convolutional neural networks. In *Proc. NIPS*, 2012. 1, 2
- [12] A. Levin, Y. Weiss, F. Durand, and W. T. Freeman. Understanding and evaluating blind deconvolution algorithms. In *Proc. CVPR*, 2009. 2
- [13] T.-Y. Lin, M. Maire, S. Belongie, J. Hays, P. Perona, D. Ramanan, P. Dollár, and C. L. Zitnick. Microsoft COCO: Common objects in context. In *Proc. ECCV*, 2014. 7
- [14] T. Michaeli and M. Irani. Blind deblurring using internal patch recurrence. In *Proc. ECCV*, 2014. 2
- [15] M. Mostajabi, P. Yadollahpour, and G. Shakhnarovich. Feed-forward semantic segmentation with zoom-out features. In *Proc. CVPR*, 2015. 1, 2, 7, 8
- [16] X. Peng, J. Hoffman, S. X. Yu, and K. Saenko. Fine-to-coarse knowledge transfer for low-res image classification. In *Proc. ICIP*, 2016. 3
- [17] S. Ren, K. He, R. Girshick, and J. Sun. Faster R-CNN: Towards real-time object detection with region proposal networks. In *Proc. NIPS*, 2015. 1, 2
- [18] C. J. Schuler, H. C. Burger, S. Harmeling, and B. Scholkopf. A machine learning approach for non-blind image deconvolution. In *Proc. CVPR*, 2013. 2
- [19] C. J. Schuler, M. Hirsch, S. Harmeling, and B. Schölkopf. Learning to deblur. *PAMI*, 2014. 2
- [20] K. Simonyan and A. Zisserman. Very deep convolutional networks for large-scale image recognition. In *Proc. ICLR*, 2015. 1, 2, 3, 4
- [21] C. Szegedy, W. Zaremba, I. Sutskever, J. Bruna, D. Erhan, I. Goodfellow, and R. Fergus. Intriguing properties of neural networks. In *Proc. CVPR*, 2014. 3
- [22] S. Ullman, L. Assif, E. Fetaya, and D. Harari. Atoms of recognition in human and computer vision. *PNAS*, 2016. 3
- [23] L. Xu, J. S. Ren, C. Liu, and J. Jia. Deep convolutional neural network for image deconvolution. In *Proc. NIPS*, 2014. 2
- [24] D. Zoran and Y. Weiss. From learning models of natural image patches to whole image restoration. In *Proc. ICCV*, 2011. 2